

CAAP Quarterly Report

December 20, 2024

Project Name: Determination of Potential Impact Radius for CO₂ Pipelines using Machine Learning Approach

Contract Number: 693JK32250011CAAP

Prime University: Texas A&M University

Prepared By: Sam Wang, qwang@tamu.edu, 979-845-9803

Reporting Period: 9/27/2024 – 12/26/2024

Project Activities for Reporting Period:

The following relevant tasks in the proposal have been completed:

- Held the third TAP meeting with PHMSA representatives.
- Studied the simulation results and conducted the case studies to address the questions mentioned in the TAP meeting on Nov 7, 2024. More details are provided in the appendix.
- Studied the evacuation time of plain terrain. More details are provided in the appendix.

Project Financial Activities Incurred during the Reporting Period:

Based on the proposed budget, the cost is broken down into two parts:

- Efforts from the PI Dr. Wang for about 0.25 month.
- Efforts and work by graduate students, Chi-Yang Li and Jazmine Aiya D. Marquez, totally for about 2 months for each of them.

Project Activities with Cost Share Partners:

Dr. Wang's time and efforts (0.25 month) in this quarterly period are used as cost share. He devoted his time to supervising the graduate students, review all results, organize the third TAP meeting, prepare and submit the progress report.

Project Activities with External Partners:

Request to participate in the Skylark Joint Industry Project (JIP) was forwarded to PHMSA office for a final approval. Reasons and justifications for non-competitive funding to extend this project were submitted.

Potential Project Risks:

None.

Future Project Work

- Study the evacuation time for medium hill, big hill, medium valley, and big valley terrains.
- Develop a web-based tool to determine the PIRs for CO₂ pipelines and evacuation times.

Potential Impacts to Pipeline Safety:

- The variables for pipeline characteristics and weather conditions cover the upper limits and lower limits of the current industrial practices; therefore, the machine-learning model is believed to have accurate predictions for other CO₂ pipelines in the range.

Appendix

1. Statistics for simulation results

Table 1 presents the mean distance of dispersion for three concentration levels across five terrain types simulated in Ansys Fluent. Generally, flat terrain exhibits the farthest dispersion, followed by medium valley, medium hill, big valley, and big hill.

Table 1. Mean of distance for three levels of concentrations for five types of terrain.

Terrain	Mean of distance for 9% CO ₂ (m)	Mean of distance for 4% CO ₂ (m)	Mean of distance for 1% CO ₂ (m)
Flat	115.4	241.0	1083.3
Medium Hill	98.4	192.2	801.5
Big Hill	81.5	153.8	559.5
Medium Valley	98.8	258.2	971.2
Big Valley	85.9	144.7	642.2

2. Case studies: Valley with flat bottom & Flat terrain with vertical release

According to the TAP meeting on November 7, 2024, there was a discussion on the reason why the flat terrain could reach farther than valley terrain (Table 1). Since the base of the valley terrain acquired is sloped rather than flat, we conducted a case study on a valley with a flat bottom – similar to a canyon – which is an uncommon location for pipelines. This will allow us to understand if the bottom of the valley affects the dispersion distances.

Given that many CO₂ pipelines are buried, a scenario of concern involves the pipeline explosion creating a crater; with the release from both ends of the ruptured pipeline converging and escaping upward from the crater. In our simulations, we doubled the mass flow rate to approximate the release from both ends of a ruptured pipeline, creating the dataset.

Consequently, we conducted an additional case study by orienting the virtual pipeline vertically relative to the terrain.

For the former, the terrain for simulation is a section from the Grand Canyon. For latter, the crater is created on the flat terrain. Meanwhile, the results from flat terrain and medium valley are also collected to compare with the results from case studies. Furthermore, the parameters for the simulation are shown in Table 2.

Table 2. Parameters applied for study.

Pressure (MPa)	Diameter (inch)	Flow rate (MMcfd)	Wind speed (mph)	Temperature (°F)
10	30	1300	3	100

With the help of Ansys Fluent to prepare data and PyVista to visualize the data, the elevation contours for the cases are shown from Figure 1 to Figure 4, and mole fraction of CO₂ contours for the cases are shown from Figure 5 to Figure 8. Additionally, the diagram of CO₂ mole fractions versus distances under 1000 meter and that between 1000 and 2000 meter are shown as Figure 9 and Figure 10.

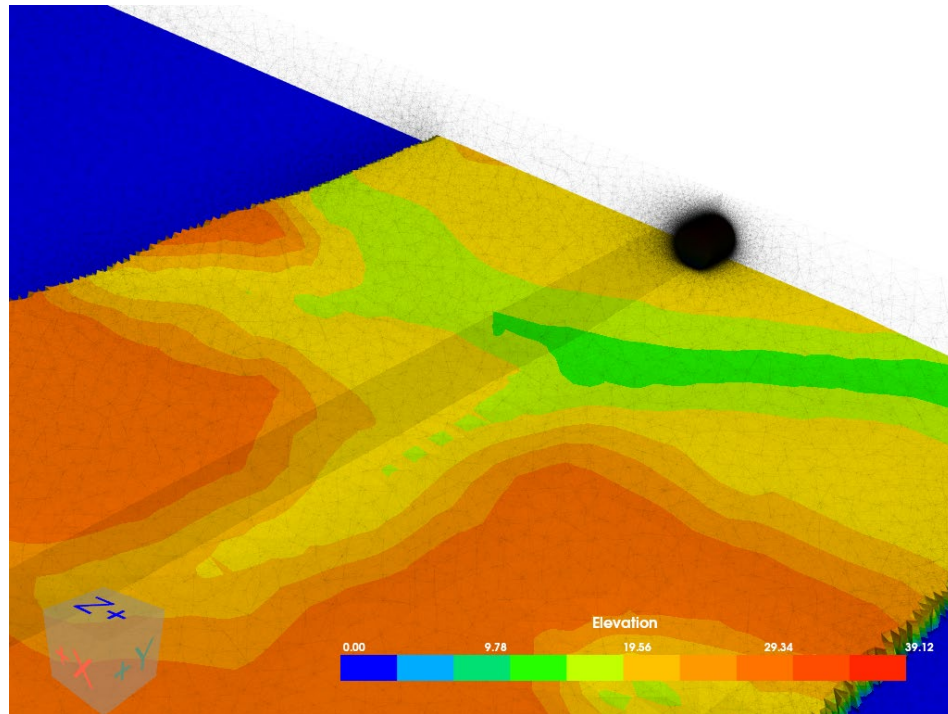


Figure 1. Elevation contours for original flat terrain.

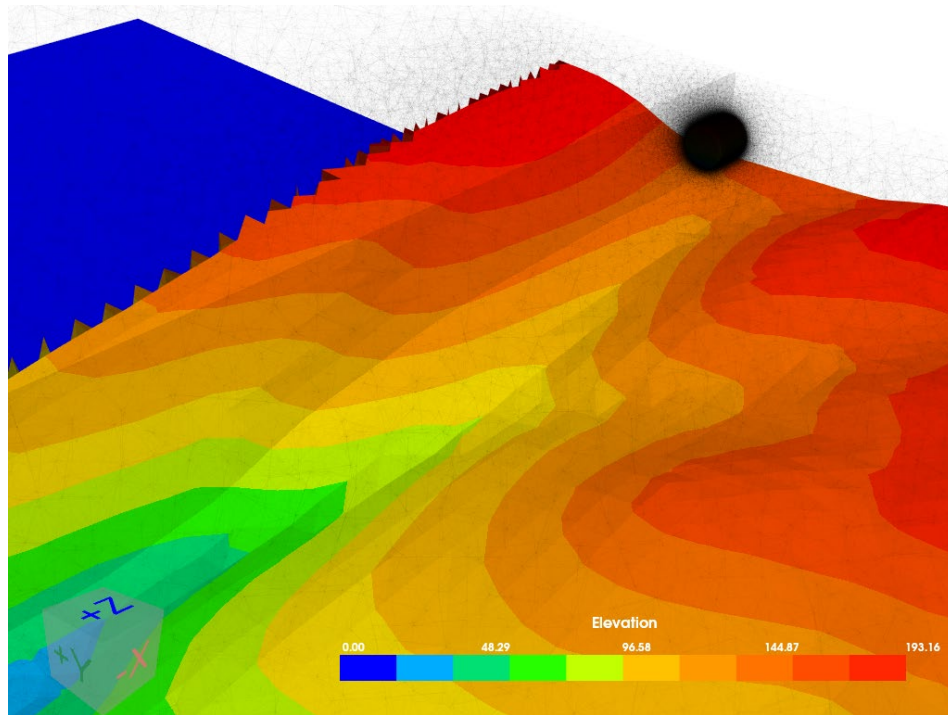


Figure 2. Elevation contours for original medium valley terrain.

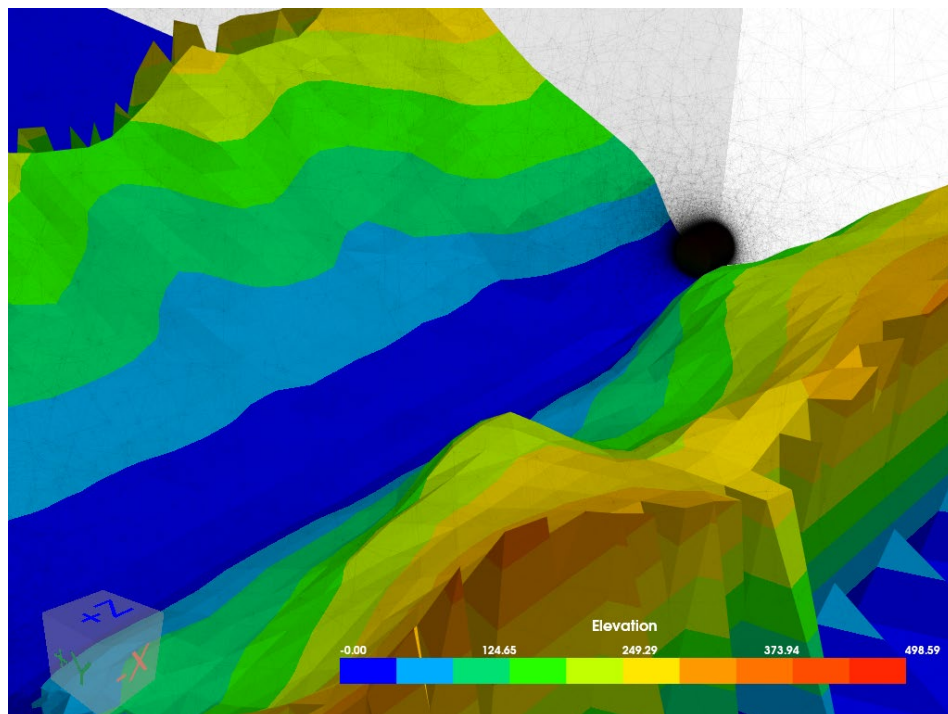


Figure 3. Elevation contours for valley terrain with flat bottom.

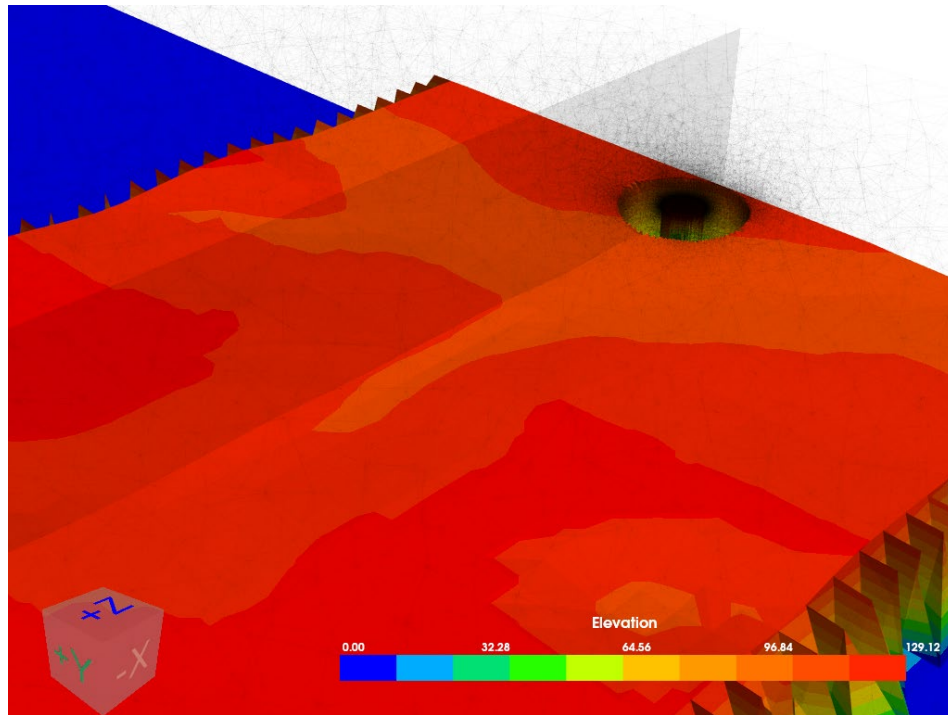


Figure 4. Elevation contours for flat terrain with vertical release.

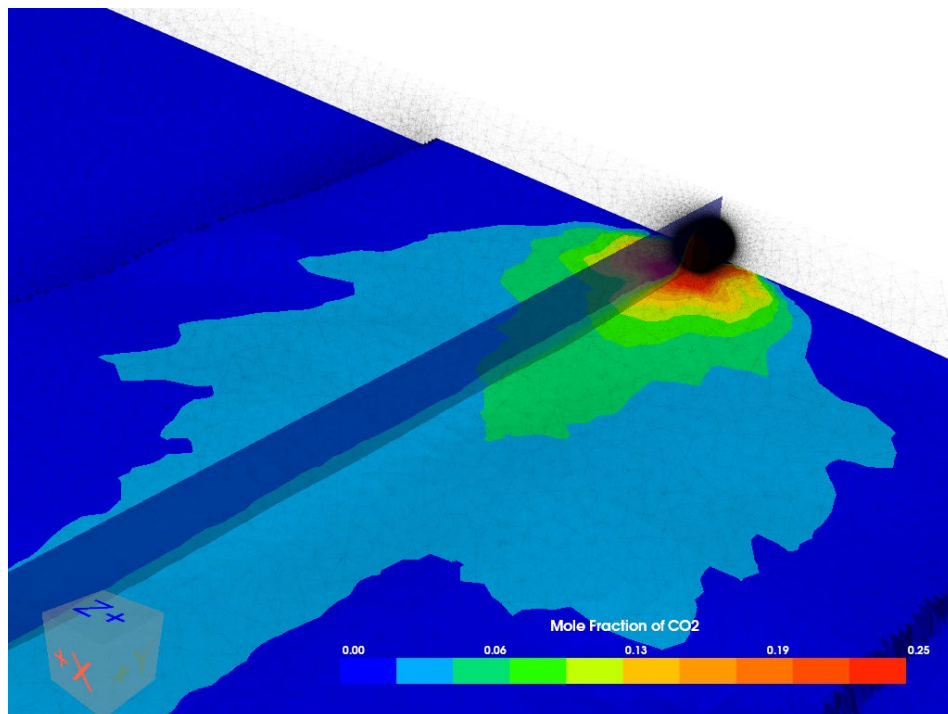


Figure 5. Mole fraction of CO₂ contours for original flat terrain.

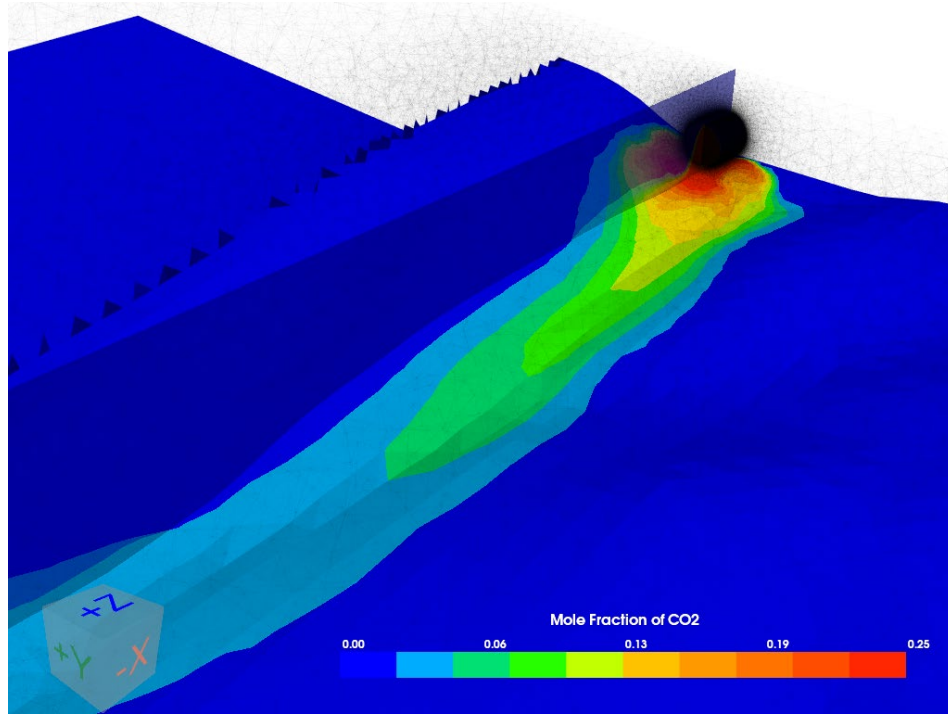


Figure 6. Mole fraction of CO₂ contours for original medium valley terrain.

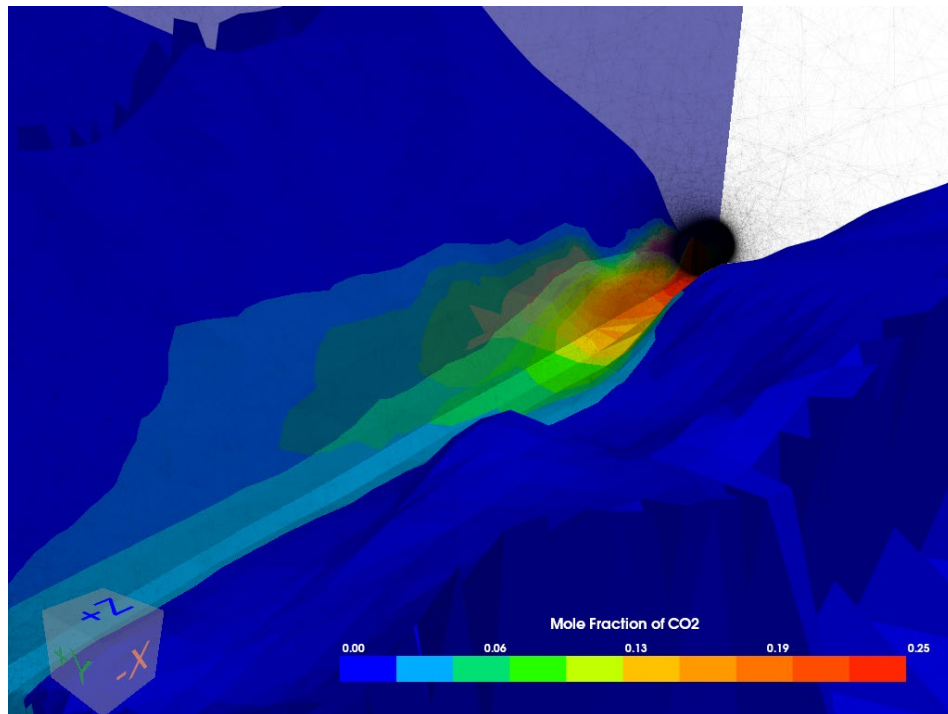


Figure 7. Mole fraction of CO₂ contours for valley terrain with flat bottom.

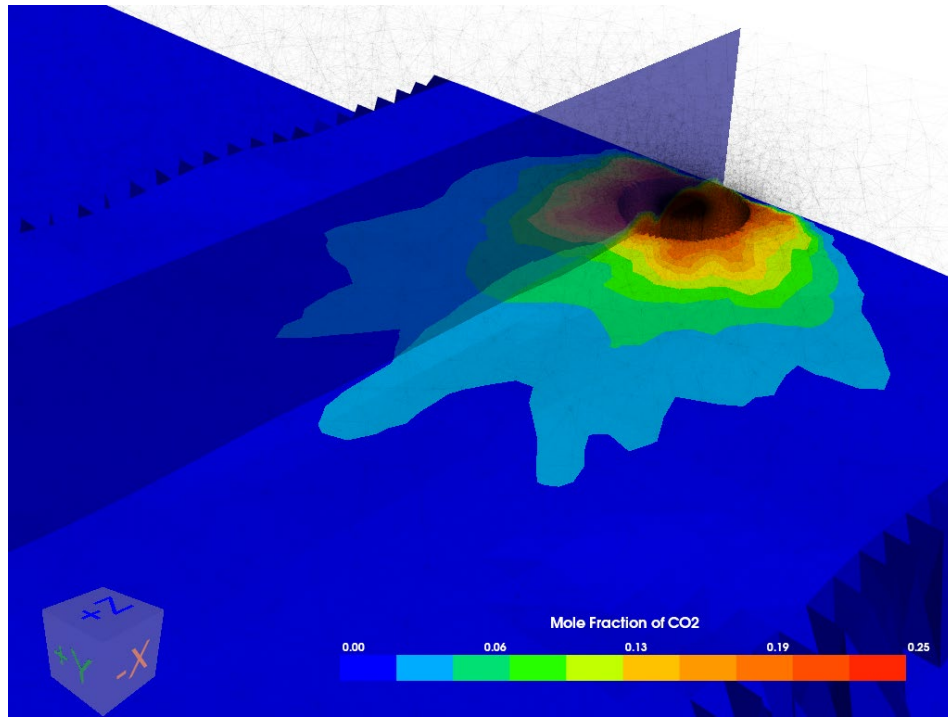


Figure 8. Mole fraction of CO₂ contours for flat terrain with vertical release.

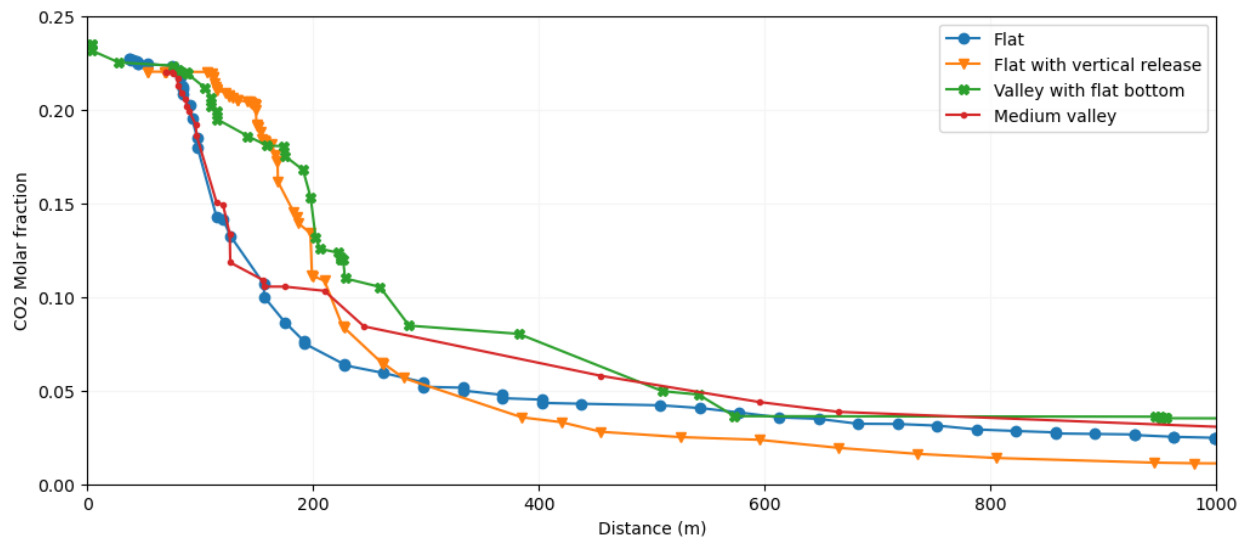


Figure 9. CO₂ mole fraction versus distance under 1000 meters.

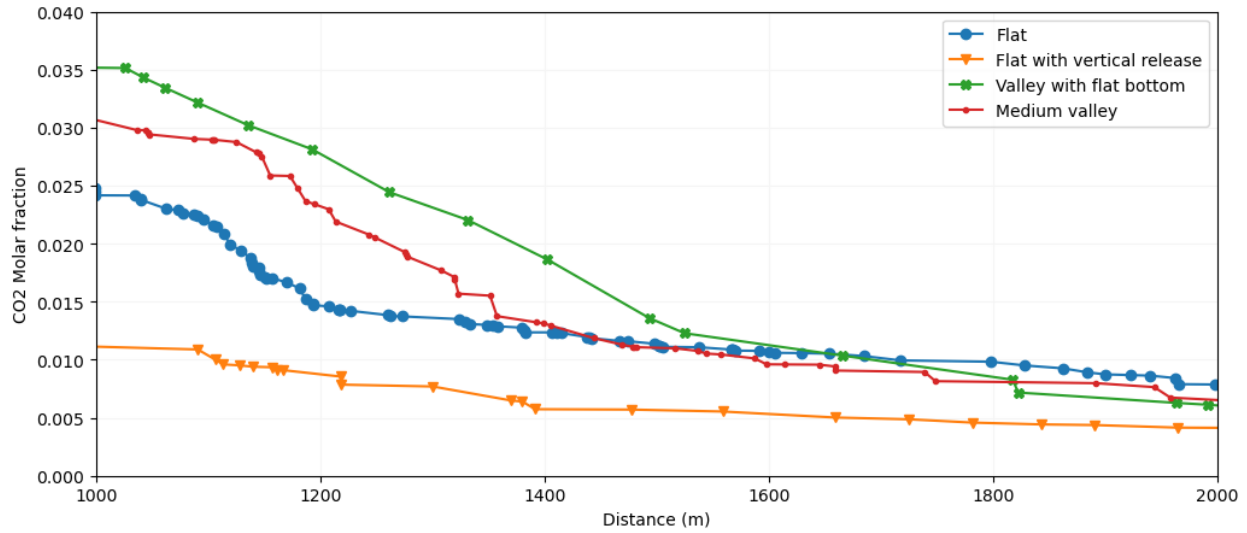


Figure 10. CO₂ mole fraction versus distance between 1000 and 2000 meters.

As shown in Figure 9, the flat terrain with vertical release exhibits the highest concentration initially, but it decreases rapidly around 150 meters, eventually becoming the lowest at approximately 300 meters and maintaining this ranking until the end. Beyond 300 meters, the valley with a flat bottom generally exhibits the highest values up to 1700 meters, followed by the medium valley, as shown in Figure 9 and Figure 10. In contrast, the CO₂ molar concentration for the flat terrain decreases rapidly initially but more gradually over time. Ultimately, it becomes the highest value at 1700 meters.

From the case studies, we can conclude that the medium valley and the valley with flat bottom share similar results, and the latter generally has slightly higher values. Thus, the flat bottom would increase the dispersion distances. However, the flat terrain still holds the farthest distance on the 1% CO₂ molar concentration. Therefore, the valley terrain holds higher concentrations at shorter distances, while the flat terrain can reach farther. On the other hand, for the flat terrain with vertical release, except for the concentration before 300 meters, it consistently maintains a higher concentration. Since the release from both ends of the ruptured pipeline may not be perfectly upward, the assumption of converging release in the same direction as the wind could be considered as the worst-case scenario.

3. Case study: Lower ambient pressure

There was also a question regarding the influence of ambient pressure at higher elevation locations. According to previous reports, near-field dispersion is simplified using analytical solutions by considering thermodynamics and Peng-Robinson equations of state, followed by CFD simulations for far-field dispersion. The influence of lower ambient pressure is considered in the near-field calculations. For the CFD simulations, the parameters of concern are terrain type, wind speed, ambient temperature, far-field velocity, far-field radius, and distance for reaching ambient temperature and pressure. Among them, ambient pressure would affect far-field velocity, far-field radius, and distance for reaching ambient temperature and pressure.

The major U.S. city with the lowest ambient pressure, which is around 83–85 kPa, is Denver, Colorado. With the input from Table 2, the results of near-field calculations are shown in Table 3. Additionally, the correlation matrix considering the parameters of concern in CFD simulations based on all the simulations is Figure 11, except for terrain type, which cannot be easily represented by a numerical value. Among them, distance for reaching ambient temperature and pressure and far-field radius are relatively important parameters for dispersion distances. Given that the differences between these variables are small, the influence of ambient pressure caused by higher elevation is limited.

Table 3. Comparison of different ambient pressures.

Ambient pressure (kPa)	Far-field velocity (m/s)	Far-field radius (m)	Distance for reaching ambient temperature and pressure (m)
101.325	2.26	17.17	48.86
84	2.27	18.85	53.67

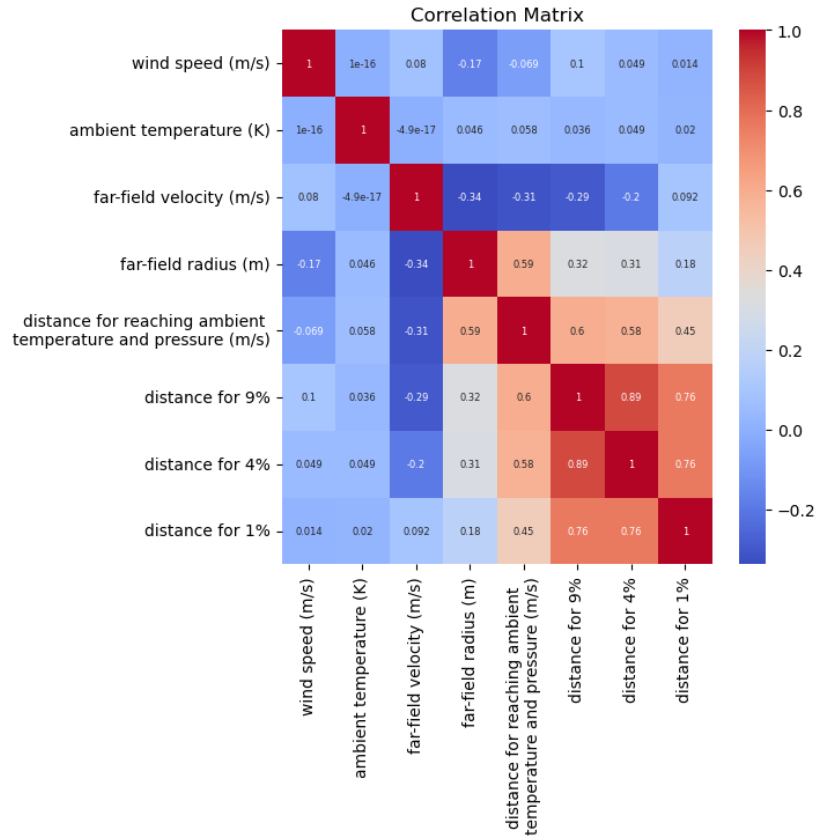


Figure 11. Correlation matrix for the parameters of concern.

4. Evacuation time for releases in plain terrain

As discussed in the previous report, to assess the time to reach steady state, the case with the farthest dispersion was used and the corresponding parameters are enumerated in Table 4 and results are shown in Figure 12.

Table 4. Parameters applied for study.

Pressure (MPa)	Diameter (inch)	Flow rate (MMcfd)	Wind speed (mph)	Temperature (°F)
10	30	1300	25	60

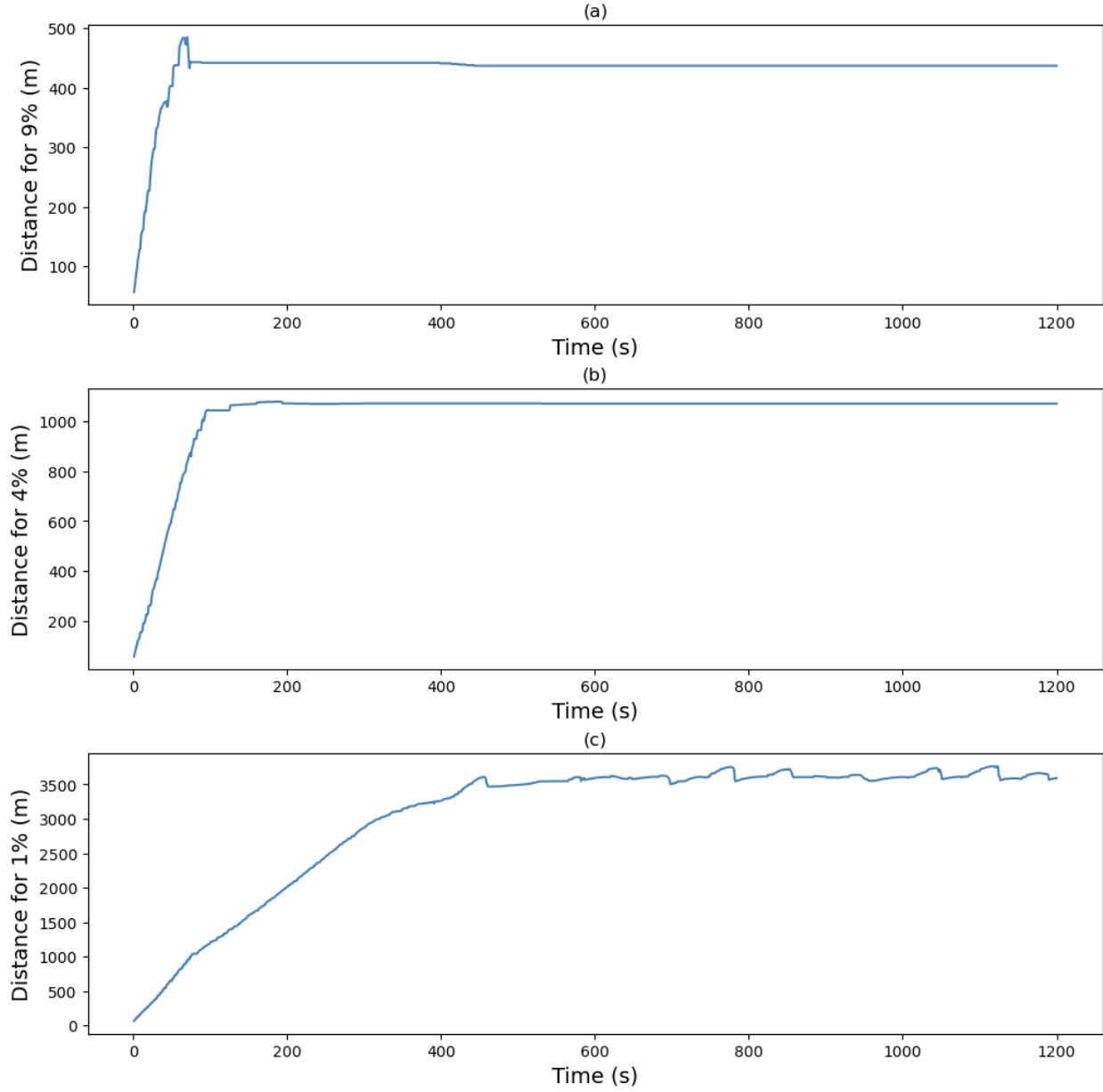


Figure 12. Distances of CO₂ concentration versus time: (a) 9%, (b) 4%, and (c) 1%.

Based on the information from the studies, the equation was developed to calculate the time (t) to reach 1%, 4%, and 9% CO₂ concentrations:

$$t = \left(\frac{D}{w}\right)^{1.045} - 0.116 * \left(\frac{D_{ss} - D}{w}\right)$$

Where, D represents the distance of concern (m), w represents wind speed (m/s), and D_{ss} represents the distance for steady state, which equals to the PIR number.

The comparison of the actual values versus the predicted values are shown in Figure 13 with R^2 of 0.986.

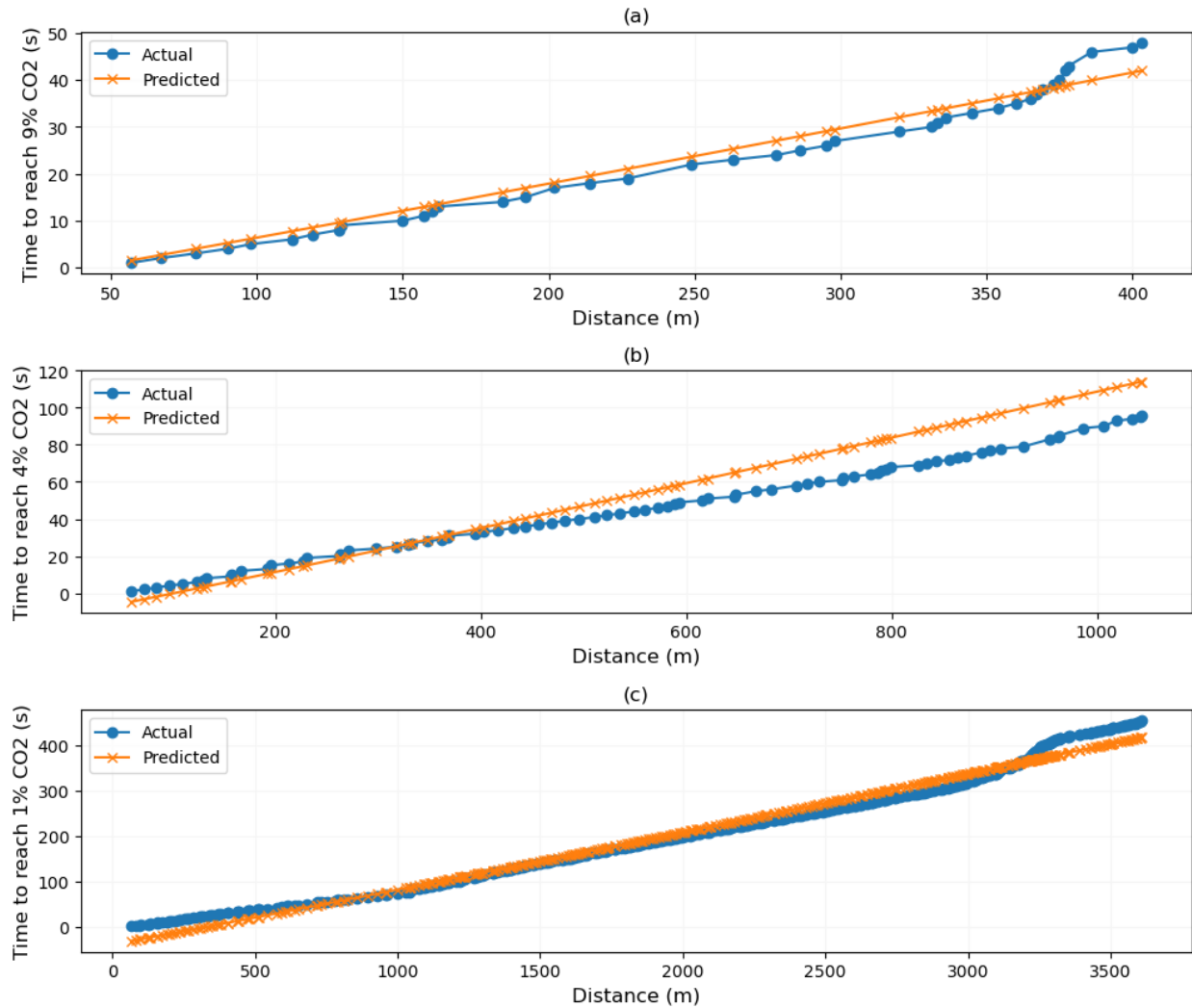


Figure 13. Actual values versus predicted values (a) 9 % CO₂, (b) 4 % CO₂, and (c) 1 % CO₂.

The equation is based on the transient simulation for the flat terrain. The transient simulation will be conducted on other terrain types and the corresponding equation to calculate the time to response will be created accordingly in the future work.